# A $z$ Plane Lerner Switched-Capacitor Filter

C. ANDREW LISH, MEMBER, IEEE

*Abstract*—**This paper discusses the design of a switched-capacitor filter that optimizes both amplitude and phase response simultaneously. Conceptually derived from a Lerner function, the filter architecture is efficient and simple.**

## SUMMARY

IN 1964 Lerner [1] described a passive filter with linear phase in the passband and sharp cutoff skirts in the stopband. The transfer function of this filter type inherently optimizes phase and amplitude response without having to add any all-pass sections for delay correction. This is significant because it was previously thought impossible to have sharp amplitude and linear phase response together due to the minimum phase design criteria. When a nonminimum phase design is performed, optimization of both a closely rectangular amplitude and linear phase response can be achieved. Lerner's original filters were fabricated with passive devices; however, as active filters became popular, others have performed the design using active devices [2], [3]. In present high performance data communications, it is necessary to have sharp amplitude response to define signal channels as well as constant group delay over the channel to prevent distortion of the data waveform, so that appropriate information can be extracted. Linear phase response with these criteria is of course necessary. Hence, we have modernized the Lerner filter by reworking the $s$ plane transfer function, converting it to the $z$ plane, and deriving and implementing an integrated switched-capacitor filter (SCF) with bandpass response. A further advantage of this filter is that the architecture is parallel, potentially resulting in faster settling times than a cascaded network. Additionally, it is relatively simple to design an SCF using these structures, and they can therefore reduce design cycle time. This building block can be used in an automated filter design CAD package.

## BACKGROUND

Two representations of transfer functions are common. The most widely used is the cascaded function.

$$H(s)=\frac{(s-z_1)(s-z_2)(s-z_3)\cdots(s-z_n)}{(s-p_1)(s-p_2)(s-p_3)\cdots(s-p_m)}. \quad (1)$$

Manuscript received June 15, 1984; revised August 3, 1984.

The author is with the Standard Microsystems Corporation, Hauppage, NY 11788.

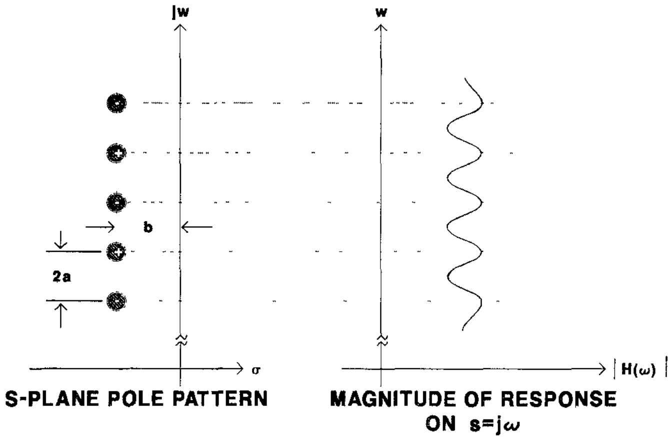


Fig. 1

Normally, the cascaded form is broken up into biquadratic sections of complex poles and/or zeros for ease of implementation. Less popular is the pole residue function; this representation is based on a summation of weighted poles and therefore no zeros need to be accounted for.

$$H(s)=\frac{r_1}{(s-p_1)}+\frac{r_2}{(s-p_2)}+\frac{r_3}{(s-p_3)}+\cdots\frac{r_n}{(s-p_n)}. \quad (2)$$

Additionally, this form will usually lead to a parallel circuit implementation of the function.

An infinite Lerner function is shown in (3). Notice that the numerator, or residues, are of alternating polarity and of equal weight. The poles are all to the left and parallel to the $jw$ axis in the $s$ plane as shown in Fig. 1 along with the constant magnitude with a slight ripple response.

$$H(s)=\sum_{-\infty}^{\infty}\frac{b(-1)^n}{s-2jna+b}. \quad (3)$$

Equations (4) and (5) represent this magnitude response as well as the closely linear (with slight ripple) phase response. By adjusting the $b/a$ ratio, the $k$ variable or ripple variable is set to the desired tolerance.

$$|H(\omega)|\approx(\pi bk/a)\left(1+k^2\cos(\pi\omega/a)+\cdots\right) \quad (4)$$

$$\phi\approx-\left[\omega\pi/2a+k^2\sin(\pi\omega/a)+\cdots\right] \quad (5)$$

$$k=e^{-\pi b/2a}. \quad (5a)$$

In our filter $a = b = 523.5988$ rads/s. The transition from passband to stopband occurs where the infinite series (3) is truncated at the desired points. Corrector poles are added to smooth the transition region spaced distance $a$ away from the boundary poles. These corrector poles more accurately set the transition points when they are used; the transition boundaries occur at the $jw$ position of the corrector poles. Equation (6) represents the truncated Lerner function.

$$H(s) = \overbrace{\sum_{k=n_L}^{n_h}\left[\frac{b(-1)^k}{s-j2ka+b}+\frac{b(-1)^k}{s+j2ka+b}\right]}^{\text{main pole-residues}} \pm$$

$$\begin{array}{c}\text{corrector}\\ \text{pole}\\ \text{residues}\end{array}\left\{\begin{array}{l}\left(\dfrac{b/2}{s-j(2n_h+1)a+b}+\dfrac{b/2}{s+j(2n_h+1)a+b}\right)\pm\\[2ex] \left(\dfrac{b/2}{s-j(2n_L-1)a+b}+\dfrac{b/2}{s+j(2n_L-1)a+b}\right).\end{array}\right. \tag{6}$$

## SYNTHESIS

To realize (6) we first group all conjugate pair terms together and factor out a common first-order term $(s+b)/s$, as shown below.

$$H(s) = \frac{s+b}{s}2\left[\overbrace{\sum_{k=n_L}^{n_h}\left(\frac{bs(-1)^k}{(s-j2ka+b)(s+j2ka+b)}\right)}^{\text{bandpass "main pole-residue"}}\pm\right.$$

$$\begin{array}{r}\text{bandpass}\\ \text{"corrector}\\ \text{pole-}\\ \text{residues"}\end{array}\left\{\begin{array}{l}\dfrac{(b/2)s}{(s-j(2n_h+1)a+b)(s+j(2n_h+1)a+b)}\pm\\[2ex] \left.\dfrac{(b/2)s}{(s-j(2n_L-1)a+b)(s+j(2n_L-1)a+b)}\right]\end{array}\right. . \tag{7}$$

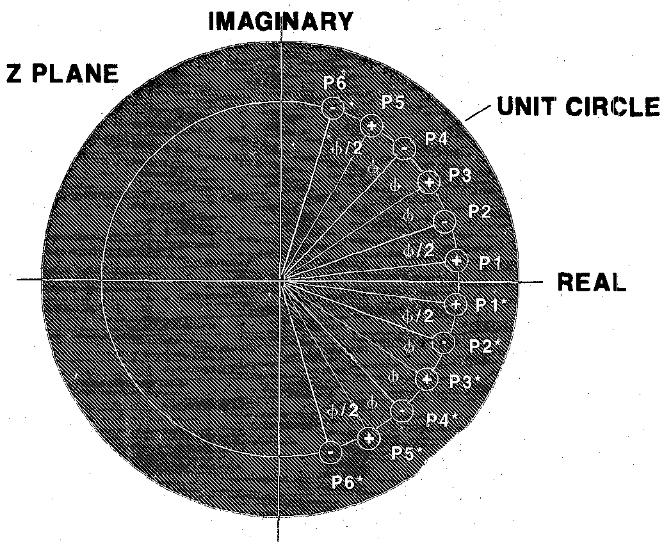


Fig. 2. $z$ plane pole residue plot.

For a switched-capacitor filter implementation of (7), we can go into the $z$ plane provided that care is taken to assure that no continuous feed-through paths exist in the overall network. Additionally, when we go into the $z$ plane, it is desirable to preserve the same geometrical sense that the $s$ plane function has: when the Fourier transform is taken in the $s$ plane by going along the $jw$ axis, poles are "passed by" at equal intervals (except the corrector poles). Likewise, when the Fourier transform is taken in the $z$ plane, by going along the unit circle's circumference, we want to "pass by" poles at equal intervals or angles. Using the matched $z$ transform [4] we perform the mapping from (7) to (8) and therefore achieve our geometrical objective.

Notice that all the summed terms have now been turned into standard second-order bandpass functions, which can be implemented separately and combined in a summing network. The first-order term will only attenuate the complete summation and not alter the frequency response as long as its zero is kept away from the band edge of the filter to be realized.

$$H(z) = \frac{1-e^{-b\tau}z^{-1}}{1-z^{-1}}2\left[\overbrace{\sum_{k=n_L}^{n_h}\left(\frac{b(-1)^k(1-z^{-1})}{(1-e^{-b\tau}e^{j2ka\tau}z^{-1})(1-e^{-b\tau}e^{-2ka\tau}z^{-1})}\right)}^{\text{bandpass "main pole-residue"}}\pm\right.$$

$$\begin{array}{r}\text{bandpass}\\ \text{"corrector}\\ \text{pole-}\\ \text{residues"}\end{array}\left\{\begin{array}{l}\dfrac{(b/2)(1-z^{-1})}{(1-e^{-b\tau}e^{j(2n_h+1)a\tau}z^{-1})(1-e^{-b\tau}e^{-j(2n_h+1)a\tau}z^{-1})}\pm\\[2ex] \left.\dfrac{(b/2)(1-z^{-1})}{(1-e^{-b\tau}e^{j(2h_L-1)a\tau}z^{-1})(1-e^{-b\tau}e^{-j(2n_L-1)a\tau}z^{-1})}\right]\end{array}\right. . \tag{8}$$

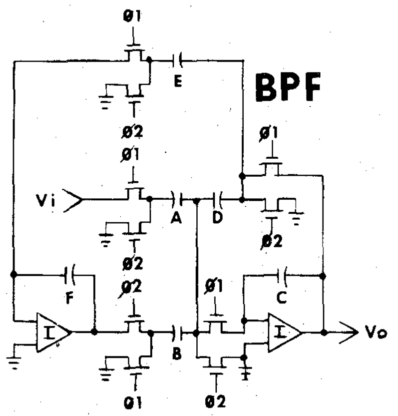


$$H(z) = -FA \frac{1 - z^{-1}}{CFz^{-2} + (BE - FD - 2CF)\,z^{-1} + FD + CF}$$

Fig. 3. Bandpass biquad.

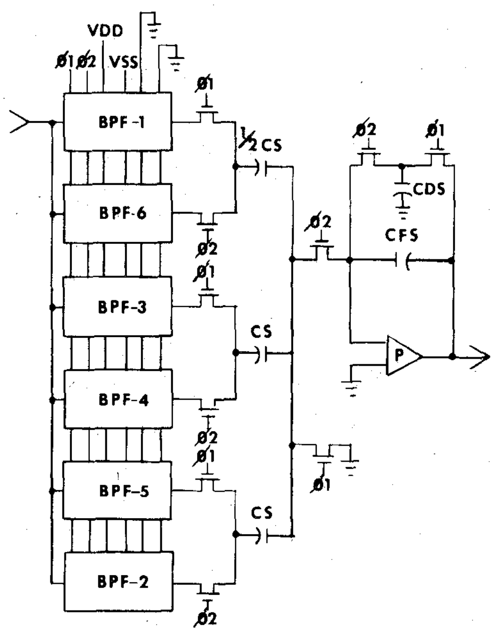


Fig. 4. Complete filter. (Patent pending.)

The active poles are arranged on a circle concentric to the unit circle spaced at equal angles with exception to the corrector poles spaced at half-angle increments (Fig. 2). There are six complex pole pairs of the type designed on our chip. Notice that due to the simplicity of a $z$ plane Lerner function there is little need to be concerned with a continuous time prototype, as the form of the $z$ plane function is fixed. The angles of the corrector pole residue filters define the passband at $\pm f_L\tau$ and $\pm f_H\tau$ where $f_L = (2n_L - 1)a$ and $f_H = (2n_H + 1)a$. The ripple is determined by the radius of the circle the poles are on, $e^{-b\tau}$, together with the angular pole spacing $2a\tau$ of the main poles. Although (6) can be written more generally so as not to restrict the position of $f_L$, it is shown slightly simplified for clarity.

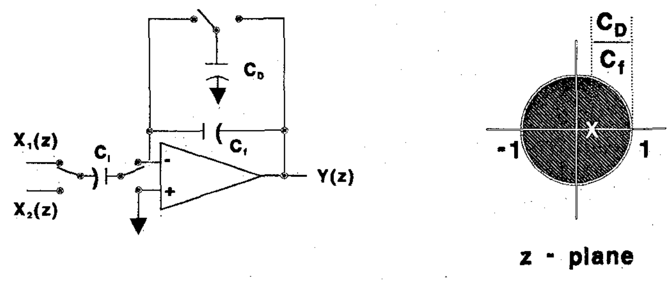


$$\frac{Y(z)}{X_1(z)} = -\frac{C_I}{C_f}\,\frac{1}{1 - z^{-1}\left(1 - \frac{C_D}{C_f}\right)}$$

Fig. 5. Summer—sample and hold.

With all the bandpass functions defined, one can now implement each of these by using a conventional biquad bandpass section [5], [6] and by matching coefficients of the $z$ transform of the biquad (Fig. 3) to those of (8). Scaling can then be performed using a simulator such as Switcap [7].

Fig. 4 shows the complete filter. Summing the bandpass functions is performed by grouping equally weighted positive and negative residue terms together and clocking them into a single capacitor at opposite clock phases. Each pair of bandpass functions is summed by a capacitor of value $C_s$, whereas the corrector pole bandpass functions are summed by a capacitor value of $1/2\ C_s$ to correspond to the needed residue values. The output of the complete filter is the sampled and held value of the summation. This is accomplished by capacitors $Cf_s$ and $Cd_s$ having virtually the same capacitance so that a previous cycle's charge stored on $Cf_s$ is "deintegrated" by $Cd_s$.

In greater detail the sample and hold is viewed as a highly dampened integrator, detailed in Fig. 5. Notice from the associated equation that when $C_d$ and $C_f$ are equal in value that the function becomes zero order, creating the desired sample and hold. Since there is a parasitic capacitance associated with $C_d$, it would be very difficult to completely match it to $C_f$; it was therefore sized to be slightly smaller than $C_f$ so that the dampening would be monotonic and not interfere with the main bandpass function.

## Implementation

Fabrication of our filter was done in a depletion-enhancement n-channel process with a minimum channel length of 8 $\mu$m for the op amp and 6 $\mu$m for all other circuits. The capacitors were formed as a polygate oxide–$n^+$ implant structure. The op amp used is similar to Tsividis' [8]. Fig. 6 shows the die photo and the filter response curves. Table I contains performance data of the device. The filter was designed to have an octave passband with a center frequency of 1 kHz with the upper and lower transition points being 666.66 and 1333.33 Hz, respectively, each occurring at $-6$ dB. These boundaries are determined by the angles of the corrector poles and by a

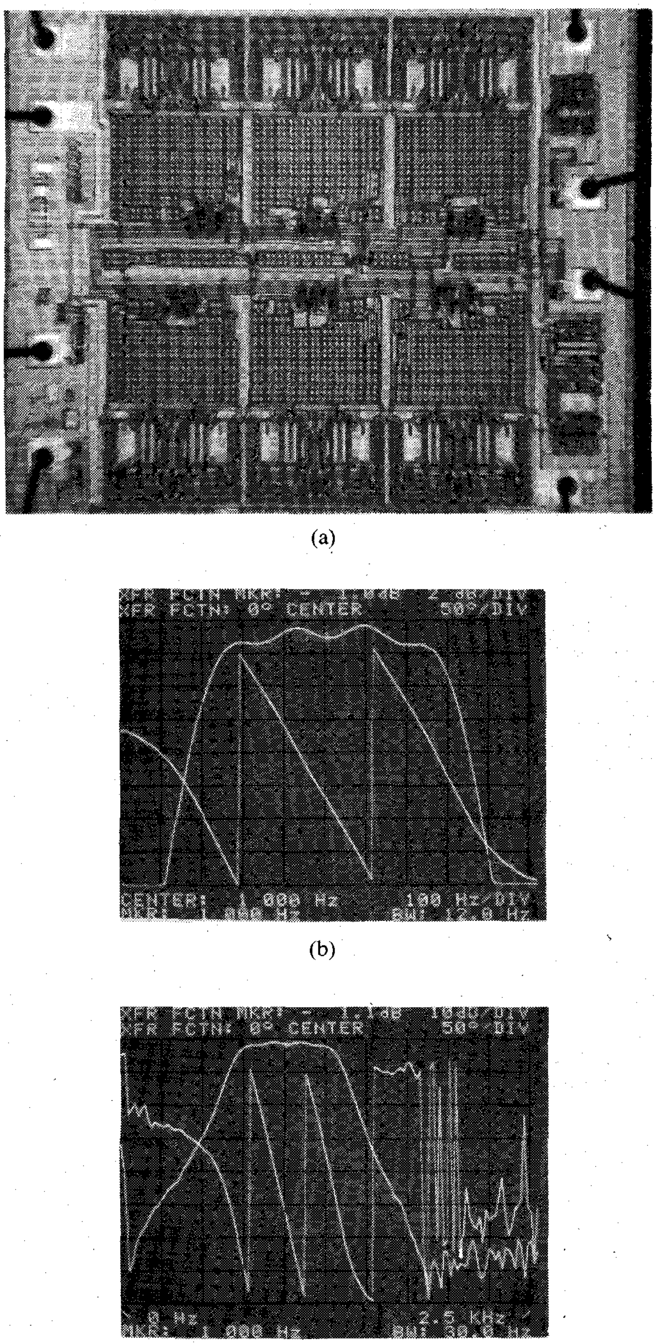


(a)

(b)

(c)

Fig. 6. Die photo and filter response curves.

clock frequency of 54.5 kHz. The angles of the corrector poles are therefore $\pm 4.404°$ and $\pm 8.807°$. The remaining four pole pairs are set in between the corrector poles, as was described earlier in the paper. All the poles are located on a circle having a radius of 0.990439. Using (4) and (5), one can derive the passband ripple magnitude $|R|$ and group delay $D(w)$

$$|R| \approx 20 \log \left[ \frac{1+k^2}{1-k^2} \right] \tag{9}$$

$$D(w) \approx \left[ \pi/2a + \frac{k^2 \pi}{a} \cos(\pi w/a) \right]. \tag{10}$$

TABLE I
FILTER SPECIFICATION

| | |
|---|---|
| Bandpass bandwidth | 1 octave bounded by 6 dB points centered |
| Clock tunable range | 10 Hz–10 kHz |
| Maximum bandpass ripple | 1 dB |
| Group delay | 3 ms $\pm$ 305 $\mu$s |
| Lower stopband slope | 0.1325 dB/Hz final stopband 70 dB |
| Upper stopband slope | 0.1438 dB/Hz |
| Average insertion loss | $-0.5$ dB |
| Passband noise | 50 $\mu V\sqrt{Hz}$ $fo = 1$ kHz; 13 $\mu V\sqrt{Hz}$ $fo = 10$ kHz |
| Output voltage swing | 4 Vp-p |
| Supply | $\pm 5$ V |
| Die size | $103 \times 108$ (mils) includes test devices |

The passband ripple for our filter was calculated to be 0.75 dB; the Switcap simulation was in tight agreement with this number, except near the band edges where the ripple increases to 1.0 dB. The error might be explained by the presence of corrector poles, whereas the (9) calculation is based on the infinite Lerner function (3). The group delay was calculated to be 3 ms with a distortion of $\pm 260$ $\mu$s; here we also saw close agreement with Switcap for the delay, but the distortion was about $\pm 305$ $\mu$s. Again, the discrepancy is probably due to the corrector poles not being accounted for in (10). Comparing the simulator output to Table I, one can see that the filter performs as was predicted by Switcap.

## Discussion

It is desirable to compare our filter to one of similar performance designed using standard techniques. An elliptic filter could be designed to match the amplitude characteristics of our filter followed by all-pass sections to equalize the group delay to an equivalent tolerance. Tight all-pass equalization is best carried out by specialized software [9] that is currently unavailable to the author. However, a filter with similar characteristics to our chip is cited in the literature and we draw a very rough comparison. A five biquad section bandpass filter (mostly elliptic) followed by five all-pass sections has been described [10]. The $-6$ dB band edges are located at approximately 675 and 1690 Hz; both the stopband rolloff and group delay distortion are reasonably similar to our filter, but the passband ripple appears to be somewhat greater in the conventional device. For comparison, we would have to extend the bandwidth of the $z$ plane Lerner filter by about 340 Hz by adding two biquad bandpass sections. This would increase the bandpass op amp count from 12 to 16. When the summing op amp is added, the total is increased to 17 op amps. Comparing this count to the 20 op amps used in the more conventional design approach, one can see less die area would be needed. Admittedly, this approximation method is very crude, but even if 2 or 4 op amps had to still be added and all the poles were reoptimized in the $z$ plane Lerner SCF to completely match the conventional approach, it would be done with bandpass sections having about half the capacitor area of all-pass sections. The design of the $z$ plane Lerner SCF is certainly less complex by comparison.

## Conclusion

A modernized $z$ plane Lerner switched capacitor filter design was presented that achieves nearly rectangular amplitude response and linear phase characteristics in a simple straightforward manner using nontraditional methods, eliminating the need for the more conventional all-pass delay correction.

## Acknowledgment

Thanks to S. Burstein, J. Popper, P. Richman, and P. Zimbelmann for making this project possible and to I. Pascual for chip layout. Thanks also to D. Ma and his team at wafer fab. Special appreciation to S. C. Fang and Y. P. Tsividis for advice and encouragement.

## References

[1] R. M. Lerner, "Band-pass filters with linear phase," *Proc. IEEE*, Mar. 1964.
[2] A. Delagrange, "Bring lerner filters up-to-date: Replace passive components with op-amps," *Electron. Des.*, Feb. 15, 1979.
[3] K. DeWitt, U. S. Patent 3 727 147, Apr. 10, 1973.
[4] L. R. Rabiner and B. Gold, *Theory and Application of Digital Signal Processing*. Englewood Cliffs, NJ: Prentice-Hall, 1975.
[5] K. Martin, "Improved circuits for the realization of switched capacitor filters," *IEEE Trans. Circuits Syst.*, Apr. 1980.
[6] P. E. Fleischer and K. R. Laker, "A family of active switched capacitor building blocks," *Bell Syst. Tech. J.*, Dec. 1979.
[7] S. C. Fang, Y. P. Tsividis, and O. Wing, "SWITCAP: A switched-capacitor networks analysis program—Part I: Basic features," *IEEE Circuits Syst. Mag.*, pp. 4–10, 1983; also see ——, "SWITCAP: A switched-capacitor network analysis program—Part II: Advanced applications," *IEEE Circuits Syst. Mag.*, pp. 41–46, Dec. 1983.
[8] Y. P. Tsividis, D. L. Fraser, Jr., and J. E. Dziak, "A process-insensitive high performance NMOS operational amplifier," *IEEE J. Solid-State Circuits*, Dec. 1980.
[9] H. J. Blinchikoff and A. I. Zverev, *Filtering in the Time and Frequency Domains*. New York: Wiley, 1976.
[10] L. T. Lin and H. Tseng, "Monolithic filters for 1200 band modems," in *ISCAS, IEEE Conf. Proc.*, 1982.

**C. Andrew Lish** (M'80) was born in New York, NY, on February 15, 1953. He received the B.S.E.E. and M.Eng.E.E. degrees from Rensselaer Polytechnic Institute, Troy, NY, in 1975 and 1976, respectively.

He has primary responsibility for the analog MOS research, development, and design effort at the Standard Microsystems Corporation, Hauppauge, NY.

# A Programmable CMOS Dual Channel Interface Processor for Telecommunications Applications

BHUPENDRA K. AHUJA, MEMBER, IEEE, PAUL R. GRAY, FELLOW, IEEE, WAYNE M. BAXTER, AND GREGORY T. UEHARA, MEMBER, IEEE

***Abstract*—A CMOS analog VLSI chip for telecommunication applications has been designed with many desirable line card features, which are programmable through a unique digital interface from the central switching office. The paper emphasizes the circuit innovations of some key analog functions realized on the chip, specifically, the operational amplifier family, the precision bandgap reference circuit, and the line balancing function. The die size of the analog VLSI is approximately 50 000 mils$^2$, and the active power dissipation is 80 mW with a 1 mW standby mode.**

Manuscript received June 15, 1984; revised August 3, 1984.
B. K. Ahuja, W. M. Baxter, and G. T. Uehara are with the Intel Corporation, Chandler, AZ 85224.
P. R. Gray is with the Department of Electrical Engineering and Computer Sciences, University of California, Berkeley, CA 94720.

## I. Introduction

The advent of single-chip codec/filter integrated circuits [1], [2] has greatly reduced the cost of per-line electronics in digital switching and transmission systems. However, one drawback of such chips has been the necessity of adding external components to the line card to perform functions such as line balancing. A second drawback has been the difficulty of adapting the line card to the specific requirements of different system applications. This paper describes a CMOS VLSI interface circuit incorporating all of the low-voltage functions for a subscriber line

0018-9200/84/1200-0892$01.00 ©1984 IEEE